Subpicosecond studies of the solvation dynamics of fluoroprobe in liquid solution

Middelhoek, E.R.; Zhang, H.; Verhoeven, J.W.; Glasbeek, M.

DOI
10.1016/0301-0104(96)00147-4

Publication date
1996

Published in
Chemical Physics

ELSEVIER

Chemical Physics 211 (1996) 489–497

Chemical Physics

Subpicosecond studies of the solvation dynamics of fluoroprobe in liquid solution

E.R. Middelhoek [a], H. Zhang [a], J.W. Verhoeven [b], M. Glasbeek [a,*]

[a] *Laboratory for Physical Chemistry, University of Amsterdam, Nieuwe Achtergracht 127, 1018 WS Amsterdam, The Netherlands*
[b] *Laboratory of Organic Chemistry, University of Amsterdam, Nieuwe Achtergracht 129, 1018 WS Amsterdam, The Netherlands*

Received 18 March 1996

Abstract

The dynamic Stokes shift of fluoroprobe in its lowest excited charge transfer state has been studied in a series of solvents, at room temperature, with a time resolution of about 300 fs. Using the fluorescent upconversion method dynamic Stokes shifts of up to 3000 cm^{-1} have been resolved. The Stokes shift is attributed to the solvent response to the large photoinduced dipole moment of fluoroprobe ($\sim$ 30 D) in the fluorescent charge transfer state. The solvation dynamics is determined by the rotational diffusional motions of the ethereal solvent molecules.

1. Introduction

In recent years numerous studies of ultrafast solvation dynamics in liquid solution have been reported. For reviews see [1–4]. In most investigations experimental information was obtained from Time Resolved Stokes Shift (TRSS) measurements [2,4]. In such experiments, pulsed photoexcitation prepares the solute molecules in an emissive excited electronic state which is not yet in equilibrium with the bath of solvent molecules. Reorientational motions of the solvent molecules give rise to the dynamic relaxation of the system. The ensuing dynamic Stokes shift is manifested as a shift with time of the frequency characteristic of the emission of the solute molecules. Probing the time behavior of this frequency shift yields the information concerning the solvation dynamics [5]. Commonly, the dynamic Stokes shift is expressed by the solvent response function given by $C(t) = (\nu_{max}(t) - \nu_{max}(\infty))/(\nu_{max}(0) - \nu_{max}(\infty))$ where $\nu_{max}(t)$ represents the frequency of the emission band maximum at time t.

Recently the time dependence of the solvent response function has been investigated to within the femtosecond time regime [4,6–11]. In a few cases the solvent response function revealed two components, a fast Gaussian-shaped component and a slower picosecond (multi-) exponential decay component (see e.g., Refs. [4,11]). The results were in remarkable agreement with the behavior first predicted by molecular dynamics simulations [12]. From these computer simulations it was inferred that the fast (Gaussian) component originates from small-angle free rotational motions of the solvent molecules in the solvent cage. For some cases it has been found that about 50% or even more of the Stokes shift is due to this inertial component [12–15]. The time scale for the inertial motions is typically in the range

* Fax: 31-20-525-6994

PII S0301-0104(96)00147-4

of 50 to 500 fs. The (multi-) exponential decay components in the solvent response function were attributed to the time-dependent diffusive-like adjustment of the orientation of the solvent dipoles to the photo-induced charge distribution at the solute molecules [2]. Typically, the time scale for the rotational Brownian motions at room temperature varies from a few picoseconds up to tens of picoseconds.

The solvation time (τ_s) characteristic of the decay of the solvent response function in the TRSS experiment is often compared with the characteristic Debye relaxation time (τ_D) as obtained from dielectric measurements for the pure solvents. Following the dielectric continuum model [16] one predicts a mono-exponential decay with $\tau_s = (\epsilon_\infty/\epsilon_0)\tau_D = \tau_l$, with ϵ_∞ and ϵ_0 being the dielectric constant at respectively infinite and zero frequency and τ_l is the longitudinal relaxation time. Although for several solutions this approximation has been found to hold (e.g., for dimethylformamide $\tau_s = 1.4$ ps and $\tau_l = 0.8$ ps [17]) more advanced modelling is necessary when deviations from the continuum theory occur.

In a recent paper we reported on TRSS experiments of the organic donor–acceptor molecule fluoroprobe (1-phenyl-4-((4-cyano-1-naphthyl)methylene)piperidine, see Fig. 1) [18]. Upon photoexcitation fluoroprobe gives rise to a broad band emission. The solvatochromism of the fluoroprobe emission has been measured in a series of solvents [19]. It appeared that the position of the emission band maximum is very sensitive to the solvent used: when changing from an apolar solvent to a very polar solvent, ν_{max} was shifted by about 8000 cm^{-1}. It was concluded that the emission is from a fluorescent charge transfer state. From time-resolved conductivity measurements [20] and optical experiments [19] the difference between the dipole moments of the ground and excited states was estimated to be approximately 30 D. Fluoroprobe is attractive for TRSS studies because of the appreciable Stokes shift of the emission of the molecule, the rather high quantum yield of its emission and also because no special solute–solvent interactions have to be considered. Our previous experiments concerned fluoroprobe dissolved in two solvents, ethylacetate and diethylether. The TRSS experiments then were performed with a time resolution of approximately 10 ps. From the ps results it was concluded that at temperatures below 200 K only the diffusive component (with typical solvation times of 10–30 ps) of the solvent relaxation process could be observed. Furthermore, it appeared that the probed solvent relaxation occurred for fluoroprobe in a pure charge transfer state unmixed with the locally excited state. Thus on a picosecond time scale fluoroprobe behaves as a pure solvation probe.

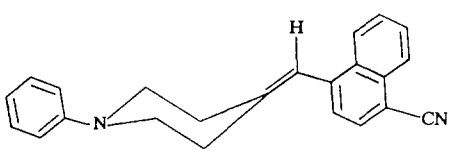

Fig. 1. Schematic picture of fluoroprobe.

In this paper we have extended our previous TRSS investigations of the solvation dynamics of fluoroprobe to shorter time scales and to two more solvents. Dynamic solvent relaxation is studied by means of the fluorescent upconversion technique with a time resolution of about 300 fs. Solvation dynamics is considered for fluoroprobe dissolved in diethylether, dibutylether, di-isopropylether and ethylacetate at room temperature. Dynamic Stokes shifts as large as 3000 cm^{-1} were resolved on a subpicosecond time scale. We emphasize that this appreciable shift for the ethereal solvents is rather exceptional: it is only due to the large dipole moment of fluoroprobe ($\sim$ 30 D) as compared to e.g., the coumarins that for the ethereal solvents the Stokes shift is more than two times the magnitude reported previously for the latter compounds [4]. Furthermore, no experimental evidence characteristic of the effects of the charge transfer process on the fluorescence intensity was obtained and it is inferred that the photo-induced intramolecular electron transfer in the electronic excited state must be complete within 300 fs after the pulsed excitation. It appears that diffusional rotational motions of the solvent molecules are responsible for the major part of the decay of the solvent response function with time.

2. Experimental

Fluoroprobe was synthesized as described elsewhere [19]. The solvents diethylether (Aldrich),

dibutylether (Aldrich), di-isopropylether (Fluka) and ethylacetate (Merck) were used without further purification. All sample preparations were carried out in a glove box to exclude oxygen and moisture. The experiments were performed with the solutions (10^{-3} M) in a 1 mm thick flow cell (upconversion experiments) or in a 1 cm quartz cuvette with two adjacent sides blackened to prevent scattering (picosecond time-correlated single photon counting measurements). In the upconversion experiments every two hours the sample was refreshed to minimize sample degradation by the laser pulses.

Time-resolved fluorescence measurements were carried out using either the femtosecond upconversion spectrometer, detailed below, with a response function of about 300 fs (FWHM) or a time-correlated single-photon counting (SPC) setup [18], with a response function of approximately 20 ps (FWHM). The use of both setups allows us to cover a time span from hundreds of femtoseconds up to nanoseconds. Steady-state absorption spectra were recorded with a Shimadzu spectrophotometer UV240; steady-state emission spectra were reconstructed from transients obtained by means of the aforementioned SPC setup. All measurements were conducted at room temperature.

The femtosecond laser system used was as follows (see also Ref. [21]). An Ar^+ laser pumped a Tsunami Ti:sapphire laser producing laser pulses with a duration of typically 60 fs ($\lambda = 800$ nm) at a repetition rate of 82 MHz and with an output energy of about 10 nJ per pulse. The femtosecond pulses seeded a regenerative amplifier (Quantronix), which consists of a stretcher/compressor system and a Nd:YLF laser to pump the regenerative Ti:sapphire amplifier. The amplifier delivered laser pulses at a repetition rate of 1 kHz and an output energy of 0.5 mJ per pulse. Part of the pulses were frequency doubled. The pulse length of the residual amplified fundamental beam is 140 fs (FWHM). The fundamental and the SH pulses were led onto a type I phase matched BBO crystal (thickness 0.2 mm) in a way that optimum overlap in space and time (by use of a variable delay line) was obtained. Thus a third harmonic (TH) pulse ($\lambda = 267$ nm) was generated. The TH pulses (~ 0.5 μJ/pulse) served to excite the fluoroprobe molecules in the absorption band. The TH beam was used as a pump beam and the fundamental-frequency beam is used as the gating beam. The time interval between the pumping and the gating pulses could be varied using an optical delay line. To avoid effects due to rotational motions of the probe molecule, all data were taken at magic angle conditions. To this end the polarization of the pump beam with respect to the gate beam was controlled by a quartz half-wave plate, set at 54.7°, in the pump arm. The TH pump beam was focused using a lens (spot size with a diameter of about 30 microns) onto the flow-cell containing the sample solution. The photo-induced fluorescence was focused together with the gating pulses (~ 0.5 μJ/pulse) onto a 1 mm BBO crystal yielding the upconverted light at the sum frequency. The upconverted emission was led through an UG11 band-pass filter and a Zeiss M20 monochromator. The sum frequencies were selected by tuning the angle of the BBO crystal as well as the monochromator wavelength. The spectral resolution of the upconverted signal is approximately 5 nm. Finally, photo-detection was by means of a photomultiplier (EMI 9863 QB/350) connected to a PAR lock-in amplifier, which was referenced by the synchronized trigger pulse delivered by the amplifier system. Data accumulation of the signal from the lock-in amplifier and data processing was accomplished by means of a personal computer. The FWHM of the measured intensity cross correlation function of the gating pulse ($\lambda = 800$ nm) and the SH pulse ($\lambda = 400$ nm), is 300 fs.

3. Results and discussion

Typical steady-state absorption and emission spectra of fluoroprobe in the four solvents diethylether, dibutylether, di-isopropylether and ethylacetate are shown in Fig. 2. The absorption spectrum of fluoroprobe in solution does not change as a function of the solvent used [19]. On the other hand, the emission spectra display solvatochromism characteristic of Lippert–Mataga behavior, i.e., the frequency of the emission band maximum, ν_{max}, varies linearly with the dielectric based solvent polarity parameter Δf [18,19]. The emission spectra of Fig. 2 display the known broad and structureless shape of the fluoroprobe emission in solution. The aforementioned spectral characteristics are illustrative of the

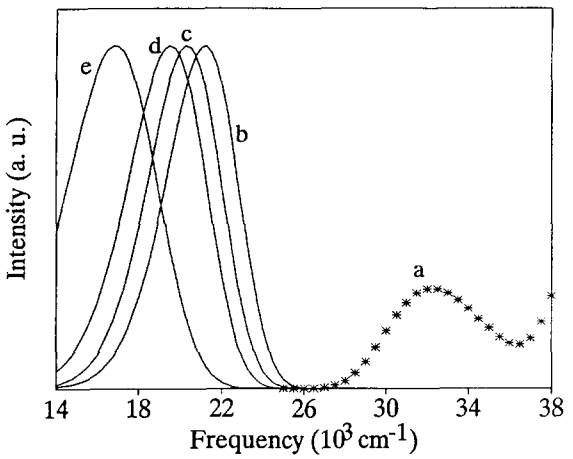

Fig. 2. (a) Steady-state absorption spectrum of fluoroprobe in diethylether at room temperature (asterisks), (b), (c), (d) and (e) corrected emission spectra of fluoroprobe in dibutylether, di-isopropylether, diethylether and ethylacetate, respectively, at room temperature (solid lines).

charge transfer state character of the fluorescent excited state. Table 1 summarizes some of the salient spectral parameters specified further below. Remark that the total Stokes shift in the steady state emission of fluoroprobe dissolved in diethyl ether is about 5100 cm^{-1} which seems significantly different from the estimated shift of 7000–8000 cm^{-1} in Ref. 18. However, it should be recalled that the latter numbers refers to the low temperature ($T \sim 160$ K) results, whereas the shifts reported here are the room temperature results.

Table 1
Emission band characteristics of fluoroprobe in the solvents ethylacetate, diethylether, di-iso-propylether and dibutylether at room temperature. ν_{max} is the frequency (in cm^{-1}) of the band maximum, b is the asymmetry parameter and Δ is the width of the log-normal fittings

	dibutyl-ether	di-isopropyl-ether	diethyl-ether	ethylacetate
ν_{max} (10^3 cm^{-1})	21.2	20.3	19.5	16.8
Stokes shift (10^3 cm^{-1}) [a]	3.4	4.3	5.1	7.8
b	−0.17	−0.15	−0.18	−0.16
Δ (10^3 cm^{-1})	4.0	4.1	4.4	5.2
quantum yield [b]	0.85	0.78	0.58	0.19

[a] Calculated by comparison with emission band in solvent n-hexane ($\nu_{max} = 24.6 \times 10^3$ cm^{-1} [18]).
[b] from Ref. [18].

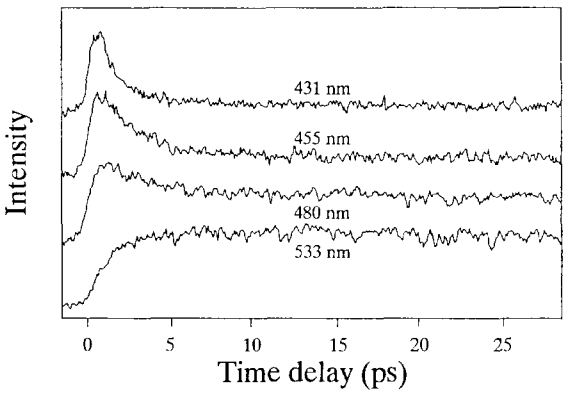

Fig. 3. Fluorescence transients of fluoroprobe in diethylether at room temperature at the emission wavelengths indicated. The transients have been measured by means of the femtosecond upconversion technique and rescaled to obtain the same maximum intensity change.

Representative fluorescence decays of fluoroprobe in diethylether on a (sub)picosecond time scale are shown in Fig. 3. Typically, for each solution, upconversion transients were measured at about ten wavelengths. The upconversion transients in Fig. 3 represent the transient fluorescence behavior during the first 25 ps after excitation. The transients give an expanded view of the initial part of the decays measured with the picosecond fluorescence setup (Fig. 4 and vide infra). As illustrated by Fig. 3, when

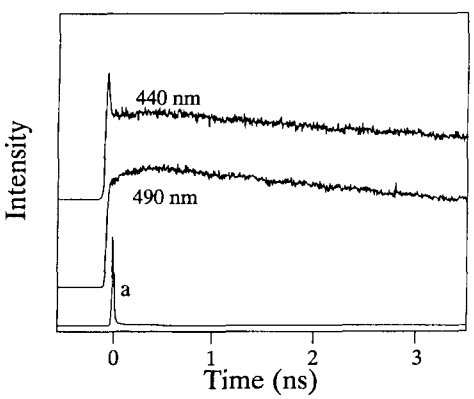

Fig. 4. Fluorescence transients of fluoroprobe in di-isopropylether at room temperature at the detection wavelengths indicated. The transients have been measured by means of the SPC setup and rescaled to obtain the same maximum intensity change. (a) represents the instrumental response function.

detection is at the blue edge of the emission band, the wavelength-dependent picosecond component initially consists of a fast subpicosecond rise and a picosecond decay. When the transient is measured more to the center of the steady-state emission band, the picosecond decay component slows down and its relative amplitude decreases. Finally, when the transients are probed at the red wing of the emission band, a picosecond rise component is monitored.

Fluorescence decays monitored by means of the picosecond fluorescence set-up were measured at only a few wavelengths in order to determine the wavelength-independent nanosecond decay component. Characteristic examples are displayed in Fig. 4. The transients in this figure are built up from two components: a wavelength-dependent picosecond component and a wavelength-independent nanosecond decay component. The amplitude of the picosecond decay component is highest when detection is on the blue edge of the spectrum; when the transients are detected at longer wavelengths the intensity of the picosecond decay component becomes less until finally at the red wing of the emission band the transient no longer can be observed. The slow (nanosecond) component is characteristic of the population decay of fluoroprobe out of the relaxed excited state to the ground state. By fitting the slow (nanosecond) component to a mono-exponentially decaying function, the characteristic lifetime of the relaxed charge transfer state of fluoroprobe in the various solutions is obtained. The resulting lifetimes are collected in Table 2.

Table 2
Fitting parameters of fluoroprobe emission band transients in ethylacetate, diethylether, diisopropylether and dibutylether at room temperature. $\nu_{max}(t)$ is fitted by a mono or biexponential function: $\nu_{max}(t) = \Sigma\, a_i \exp(-t/\tau_i) + \nu_{max}(\infty)$

	dibutyl-ether	diisopropyl-ether	diethyl-ether	ethylacetate
		Monoexp. fit		
a_1 (10^3 cm^{-1})	2.56	2.20	3.94	4.39
τ_S (ps)	12	9.1	1.5	2.7
τ_D (ps) [a]			2.4	3.1
τ_1 (ps) [a]			1.1	1.1
$\nu_{max}(\infty)$ (10^3 cm^{-1})	21.2	20.3	19.6	16.8
Stokes shift (10^3 cm^{-1})	2.56 (75%)	2.20 (51%)	3.94 (77%)	4.39 (56%)
		Biexp. fit		
a_1 (10^3 cm^{-1})		1.32	2.96	
τ_1 (ps)		5.9	1.2	
a_2 (10^3 cm^{-1})		1.21	1.21	
τ_2 (ps)		21	3.0	
$\nu_{max}(\infty)$ (10^3 cm^{-1})		20.1	19.5	
τ_{le} (ps) [b]		11	1.5	
τ_{av} (ps) [b]		13	1.7	
Stokes shift (10^3 cm^{-1})		2.52 (59%)	4.17 (82%)	
lifetime (ns)	9.7	9.4	12.4	6.5

[a] The Debye relaxation times (τ_D) and the longitudinal relaxation times (τ_1) are from Ref. [18] and references therein.
[b] The average solvation time is given as $\tau_{av} = (a_1\tau_1 + a_2\tau_2)/(a_1 + a_2)$. Percentages of the observed Stokes shifts are relative to the emission peak position for fluoroprobe dissolved in n-hexane ($\nu_{max} = 24.6 \times 10^3$ cm^{-1} [18]).

The wavelength-dependent (sub)picosecond behavior is of main interest to us. The wavelength-dependent dynamics as described above in the case of the upconversion measurements, is as expected for a dynamic Stokes shift and thus characterizes the dynamic solvation process. The spectral reconstruction method [5] was applied to obtain the time evolution of the Stokes shift from the measured transients. First, the best fit functions to the fluorescence transients measured at the whole series of detection wavelengths were obtained by fitting a trial tri-exponential function convoluted with the system response function. One of the exponential terms, representative of the nanosecond population decay out of the fluorescent state, is kept fixed during the fitting procedure. Subsequently, the integrated intensity of each transient at a certain wavelength was scaled in accordance to its relative intensity in the steady-state emission spectrum. By plotting the scaled fluorescence intensity at a certain time after the laser pulse versus the detection wavelength, the emission spectrum at that particular time was obtained. The time-resolved emission spectra were fit to a log-normal distribution function $f(\nu)$ of the form,

$$f(\nu) = \begin{cases} g_0 & \exp\left\{-\ln(2)\left(\dfrac{\ln[1+2b(\nu-\nu_{max})/\Delta}{b}\right)^2\right\} \\ & \text{if } 2b(\nu-\nu_{max})/\Delta > -1 \\ 0 & \text{else} \end{cases} . \quad (1)$$

The fits yielded the experimental behavior as a function of time of the frequency of the maximum of the

emission band (ν_{max}), the width of the log-normal shape function (Δ), the asymmetry parameter (b), the height of the emission band maximum (g_0) and the integrated intensity (I) given by:

$$I = \left(\frac{\pi}{4\ln(2)}\right)^{\frac{1}{2}} g_0 \Delta \exp\left(\frac{b^2}{4\ln(2)}\right). \quad (2)$$

It is remarked that the parameters in the log-normal shape function (i.e., g_0, b, Δ), as well as the variables (ν and ν_{max}), in fact are time dependent, e.g., $\nu(t)$, but for brevity reasons this time-dependence has not been incorporated explicitly in Eqs. (1) and (2). As an example, Fig. 5 shows a few time-resolved spectra for fluoroprobe, dissolved in ethylacetate, at room temperature. Fig. 5 illustrates that there is a shift of the position of the emission band maximum of a few thousand cm^{-1} to lower values on a picosecond time scale.

Normally, the normalized Stokes shift function $C(t)$ is considered to discuss the Stokes shift dynamics. However, it is difficult to obtain reliable experimental values for $\nu_{max}(0)$. On the other hand, the time dependence of $C(t)$ is similar to that for $\nu_{max}(t)$ thus we restrict ourselves to a consideration of the latter parameter. $\nu_{max}(t)$ was plotted as a function of the time after the excitation pulse (see Fig. 6). The

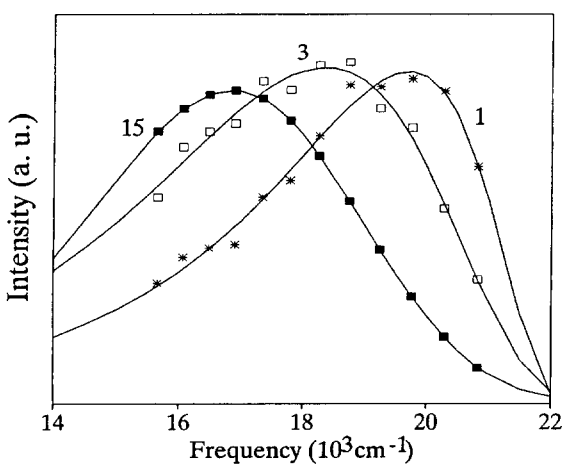

Fig. 5. Time-resolved emission spectra of fluoroprobe in ethylacetate at room temperature. The time delay of the deconvoluted spectra (in picoseconds) with respect to the pulsed excitation is as indicated. The spectra shown are log-normal functional fits to data points.

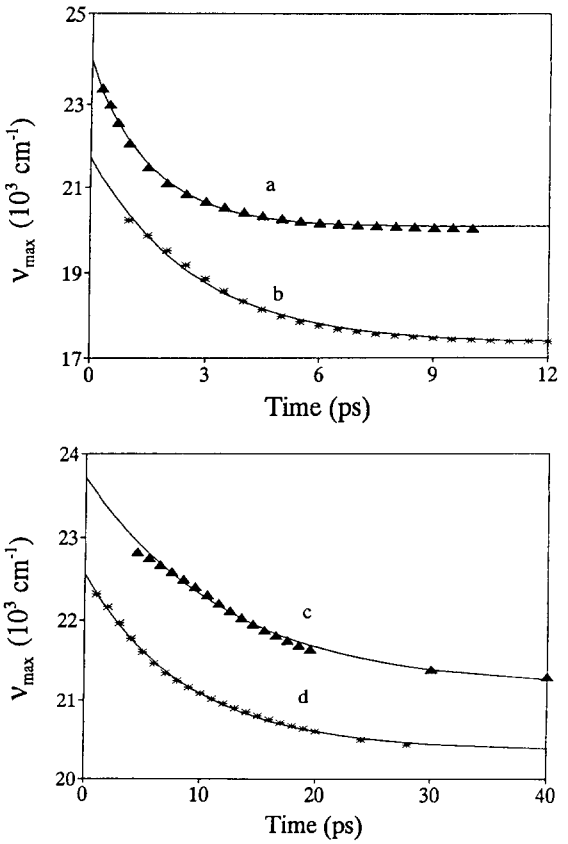

Fig. 6. Time-dependence of the frequency of the emission band maximum, ν_{max}, of fluoroprobe in diethylether (a), ethylacetate (b), dibutylether (c) and di-isopropylether (d). Solid lines are best exponential fits to data points.

plots of $\nu_{max}(t)$ as a function of time, as obtained for the various solvents, could be fitted to a mono- or bi-exponential functional decay. For the mono-exponential fit τ_s equals the time constant of this fit and for the bi-exponential fit τ_s equals the average time constant τ_{av}. The results are collected in Table 2.

Typically, for the four solvents studied $\nu_{max}(t)$ decays with solvation times in the range from 1 to 13 ps. The solvation times for the fluoroprobe/ethylacetate and the fluoroprobe/diethylether solutions are shorter than those obtained previously for the same systems at lower temperatures [18]. More specifically, in diethylether τ_s = 1.6 ps at room temperature (this work), while at temperatures ranging

from 162 to 201 K, τ_s decreases from 27 to 10 ps [18]. Thus the shorter time scale measurements are consistent with our previous results which showed that τ_s decreases as the temperature increases. For the solvents used in the current experiments, only in the case of ethylacetate our results can be compared with the ultrafast dynamics studies reported elsewhere [22,23]. The solvation times for ethylacetate obtained elsewhere [22,24] are 2.3 ps (coumarin 311) and 2.6 ps (coumarin 102), respectively. Comparing these values with the results of Table 2 it is seen that the magnitude of τ_s for fluoroprobe in ethylacetate is in good agreement with the results of Barbara's group. The fact that the solvation dynamics results for ethylacetate are independent of the solute used illustrates that specific solute–solvent interactions are of no significance and that fluoroprobe is a good solvation probe.

As mentioned in section 1, in the dielectric continuum model the solvation time τ_s equals the longitudinal dielectric relaxation time $\tau_l \approx (\epsilon_\infty/\epsilon_0)\tau_D$. In Table 2, τ_s and τ_l, as well as the Debye dielectric relaxation times τ_D, whenever available from the literature, are given for the four solvents (see also Ref. [18] and references therein). For the solvents of relevance to this work, only for ethylacetate and diethylether the τ_D values have been published. For these solvents, the solvation times, τ_s, lie in between τ_D and τ_l values. Thus the dielectric continuum model does not fully apply and improvement may be obtained with a more advanced approach, e.g., by using Fröhlich's model [16]. For the solvents dibutylether and di-isopropylether a similar comparison with the predictions of the dielectric continuum theory is not possible since dielectric relaxation measurements of pure dibutylether and di-isopropylether have, to our knowledge, not been reported.

The plots for $\nu_{max}(t)$, as determined from the time-resolved spectra, versus t do not contain an initial fast Gaussian component (cf. Fig. 6). Recently, the existence of an ultrafast Gaussian decay component in the solvent response function $C(t)$ has been predicted from molecular dynamics simulations [12]. Experimentally, the presence of an ultrafast Gaussian decay component was verified in the solvation dynamics for several small polar solvent molecules such as methanol and acetonitrile [11,23]. The Gaussian decay component, not predicted in the Debye theory for the solvent molecular motions, shows up when inertial free streaming motions of the solvent molecules in the solvent cages are taken into account. To discuss the absence of Gaussian components in our data it is first remarked that experimentally we have not been able to fully resolve the complete Stokes shift. The maximum value expected for the Stokes shift can be estimated by considering the emission spectrum at time zero. For our fluoroprobe/solvent system the absorption spectrum is independent of the solvent and for this special case the spectrum for $t = 0$ equals the emission spectrum of fluoroprobe in an apolar solvent, for example n-hexane [25]. In this way it is found that the emission band maximum at $t = 0$ is anticipated to occur for $\nu_{max}(0) = 24.6 \times 10^3$ cm^{-1} [19]. Comparison with the observed emission band frequencies immediately after the applied laser pulse then yields that about 50% of the dynamic Stokes shift has taken place when the solvent is di-isopropylether and about 30% of the dynamic Stokes shift has occurred when the solvent is diethylether. It is concluded that an appreciable part of the solvent relaxation process still remains unresolved in our experiments and this initial part may very well involve the relaxation invoked by inertial free rotational motions of the solvent molecules. For the fluoroprobe/diethylether system the presence of an ultrafast initial decay component can further be substantiated as follows. One can estimate $\omega_s^2 = \alpha_s\ \omega_F^2$, with α_s being a scaling factor determined by the dipole density and dielectric characteristics of the solvent and ω_F the free rotor frequency of the solvent molecule [26]. From microwave spectra for diethylether [27] we compute $\omega_F = 3.1$ ps^{-1}. With $\alpha_s = 1.2$, this leads to $\omega_s = 3.5$ ps^{-1} (or $t_{FWHM} = 1.8/\omega_s = 340$ fs). Keeping in mind our experimental time resolution of about 300 fs, it is not surprising that a fast solvation decay component characteristic of inertial solvent motions cannot be resolved.

We now briefly discuss the variation of the integrated emission intensity with time. As discussed recently [28], for an emissive charge transfer state the radiative decay rate constant and therefore also the total emission intensity, I, is anticipated to depend on the characteristic frequency of the optical transition. More specifically, in the conventional Mulliken two-level model [29] k_{rad} will be propor-

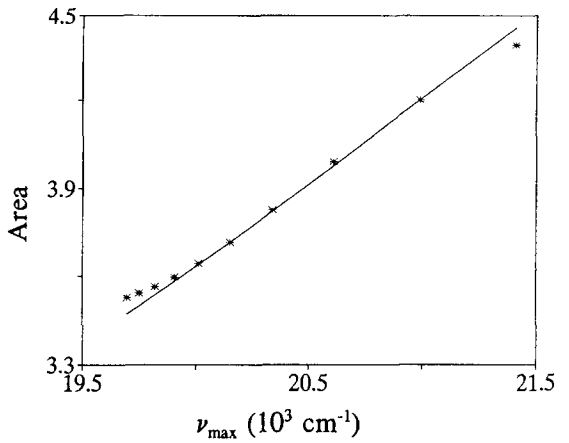

Fig. 7. Plot of integrated emission intensity, I, as a function of ν_{max} for fluoroprobe in diethylether (*). Also presented is the expected behavior of I according to the ν^3-law (solid line).

tional to ν_{max}. For a molecule like fluoroprobe an intensity borrowing mechanism has been suggested to be important, however [28]. If such intensity borrowing would be dominant, this would imply that k_{rad} is proportional to $\nu_{max}^3/[(\Delta - \nu_{max})^2 + (V^*)^2]$, where Δ denotes the energy difference between the locally excited (LE) state and the emissive charge transfer (CT) state and V^* represents the electronic coupling parameter for the coupling between the LE and CT states in the strong coupling limit. Since in the TRSS experiments presented here $\nu_{max}(t)$ was shown to decrease as time progresses, a study of $I(t)$ might provide additional information concerning the radiative mechanism for fluoroprobe. In Fig. 7, the integrated intensity of the log-normal functional fits to the experimental data is plotted as a function of ν_{max} for fluoroprobe dissolved in diethylether. Included in Fig. 7 is the best fit to the functional form, $a\nu_{max}^3$. The excellent fit shows that virtually a ν_{max}^3-law is obeyed for the fluoroprobe/diethylether system in agreement with previous measurements on a picosecond time scale [18]. When repeating the $I(t)$ measurements for fluoroprobe dissolved in ethylacetate, again a ν^3-dependence was found. (The accuracy of the measurements of $I(t)$ for fluoroprobe dissolved in di-isopropylether and dibutylether was insufficient to test its functional behavior in these cases). It thus appears that at least for the *dynamic trajectory along the potential energy curve as a function of the solvation coordinate, which is traced in the TRSS experiments of this work*, the CT state of fluoroprobe behaves as an unmixed 'pure' electronic state which follows the familiar ν^3-type behavior (i.e., Einstein's expression [30]) for spontaneous emission. It is of interest to note that previously [28], by comparing the cw emission properties of fluoroprobe in different solutions, it was argued that a $a\nu_{max}^3/[(\Delta - \nu_{max})^2 + (V^*)^2]$ dependence is likely to apply in the case of fluoroprobe. However, the ν^3-dependence found here for the behavior of fluoroprobe in single solution does not seem to support this view. When fitting the data of Fig. 7 to the functional form of $a\nu_{max}^3/[(\Delta - \nu_{max})^2 + (V^*)^2]$, a good agreement was obtained for the physically unrealistic parameter values $\Delta = 65.4 \times 10^5$ cm^{-1} and $V^* = 9.15 \times 10^6$ cm^{-1}. (The experimental data points could be also fitted to a linear function of ν (Mulliken model) but then the intercept with the ordinate axis is physically unacceptable large). Most likely, the idea that in fluoroprobe intensity borrowing as described by first order perturbation theory is dominant [28], is too simple. Eventually, the radiative decay of the probed CT state must be such that effectively, at least for the Stokes shift trajectory probed in the TRSS experiments, $k_{rad} \propto \nu^3$. $T_{CT \rightarrow DA}$, where the square of the optical transition moment, $T_{CT \rightarrow DA}$, turns out to be independent of ν.

Previously the time-dependence of the integrated intensity of the fluorescence of in a few coumarine molecules has been considered [31,32]. A ν^3-type relationship was found in case homogeneous line broadening prevails, whereas inhomogeneous line broadening effects give rise to a deviation of the ν^3 dependence. The ν^3 dependence as concluded for the time dependence of fluorescence intensities of the fluoroprobe ethereal solutions therefore reflects that the broadening of the band emission is dominated by homogeneous broadening effects.

Another feature which becomes apparent from the result that the probed fluorescence originates in a 'pure' single electronic level is that the CT state has already been formed at the earliest times experimentally accessible. Thus it is concluded that the intramolecular electron transfer kinetics is very fast and completed within the pulse duration time of 300 fs.

Finally, we want to briefly comment on the possible contribution of intramolecular vibrational relaxation (IVR) effects to the observed dynamics. A

rough estimate of the photoexcited excess vibrational energy in the excited singlet state is about 10,000 cm^{-1}. As can be seen from Table 2, the solvation time for fluoroprobe dissolved in ethylacetate is 2.7 ps. Previously, the solvation dynamics of coumarin 102, also dissolved in ethylacetate, was determined to be 2.6 ps [22,23]. In the latter experiment, the excess vibrational energy was about a few thousand cm^{-1}. We thus conclude that the solvent relaxation time for ethylacetate remains about the same regardless the nature of the solute and the amount of excess vibrational energy. Evidently, IVR for the solute molecules is much faster than the solvent relaxation times determined in the current experiments. Moreover, for a large-sized molecule such as coumarin 153 IVR occurs within a few hundred femtoseconds [4]. It is therefore not surprising that in experiments for fluoroprobe with a time resolution no better than 300 fs, not only the initial part of the dynamic Stokes shift but also IVR effects are completely missed out.

In conclusion, we have extended our previous picosecond TRSS measurements concerning the solvation dynamics of fluoroprobe, in ethereal solutions, to the subpicosecond time scale. It appears that after impulsive excitation, at room temperature, the fluorescent charge transfer state is formed within 300 fs (the time resolution of the experiments) and that the ensuing solvation dynamics does not fully comply with the dielectric continuum model. Also other ultrafast processes such as IVR and inertial free streaming motions, which may affect the initial dynamics, appear to be faster than 300 fs.

Acknowledgements

This work was supported in part by The Netherlands Foundation for Chemical Research (SON) with the financial aid from The Netherlands Organization for Scientific Research (NWO).

References

[1] K. Yoshihara, K. Tominaga and Y. Nagasawa, Bull. Chem. Soc. Jpn. 68 (1995) 696.
[2] P.F. Barbara and W. Jarzeba, Advances in photochemistry, Vol 15, ed. D.H. Volman, G.S. Hammond and K. Gollmick (Wiley, New York, 1990) p. 1.
[3] J.D. Simon, Acc. Chem. Res. 21 (1988) 128.
[4] M.L. Horng, J. Gardecki, A. Papazyan and M. Maroncelli, J. Phys. Chem. 99 (1995) 17311.
[5] M. Maroncelli and G.R. Fleming, J. Chem. Phys. 86 (1987) 6221.
[6] K. Tominaga and G.C. Walker, J. Photochem. Photobiol. A 87 (1995) 127.
[7] T. Gustavsson, G. Baldacchino and J.C. Mialocq, S. Pommeret, Chem. Phys. Lett. 236 (1995) 587.
[8] H. Zhang, A.M. Jonkman, P. van der Meulen and M. Glasbeek, Chem. Phys. Lett. 224 (1994) 551.
[9] P.J. Reid and P.F. Barbara, J. Phys. Chem. 99 (1995) 3554.
[10] D. Bingemann and N.P. Ernsting, J. Chem. Phys. 102 (1995) 2691.
[11] S.J. Rosenthal, X. Xie, M. Du and G.F. Fleming, J. Chem. Phys. 95 (1991) 4715.
[12] M. Maroncelli, J. Chem. Phys. 94 (1991) 2084.
[13] M. Maroncelli and G.R. Fleming, J. Chem. Phys. 89 (1988) 5044.
[14] E.A. Carter and J.T. Hynes, J. Chem. Phys. 94 (1991) 5961.
[15] T. Fonseca and B.M. Ladanyi, J. Phys. Chem. 95 (1991) 2116.
[16] N.E. Hill, W.E. Vaughan, A.H. Price and M. Davies, Dielectric properties and molecular behavior (Van Nostrand Reinhold Company, London, 1969).
[17] W. Jarzeba, G.C. Walker and A.E. Fleming, J. Chem. Phys. 152 (1991) 57.
[18] E.R. Middelhoek, P. van der Meulen, J.W. Verhoeven and M. Glasbeek, Chem. Phys. 198 (1995) 373.
[19] R.M. Hermant, N.A.C. Bakker, T. Scherer, B. Krijnen and J.W. Verhoeven, J. Am. Chem. Soc. 112 (1990) 1214.
[20] G.F. Mes, B. de Jong, H.J. van Ramesdonk, J.W. Verhoeven, J.M. Warman, M.P. de Haas and L.E.W. Horsman-van den Dool, J. Am. Chem. Soc. 106 (1984) 6524.
[21] P. van der Meulen, H. Zhang, A.M. Jonkman and M. Glasbeek, J. Phys. Chem. 100 (1996) 5367.
[22] M.A. Kahlow, T.J. Kang and P.F. Barbara, J. Phys. Chem. 91 (1987) 6454.
[23] S.J. Rosenthal, N.F. Scherer, M. Cho, X. Xie, M.E. Schmidt and G.R. Fleming, Ultrafast Phenomena VIII, eds. J.L. Martin, A. Migus, G.A. Mourou and A.H. Zewail (Springer,Verlag Berlin Heidelberg, 1993) p. 616.
[24] M.A. Kahlow, T.J. Kang and P.F. Barbara, J. Phys. Chem. 88 (1988) 2372.
[25] R.S. Fee and M. Maroncelli, Chem. Phys. 183 (1994) 235.
[26] M. Maroncelli, V.P. Kumar and A. Papazyan, J. Phys. Chem. 97 (1993) 13.
[27] M. Hayashi and K. Kuwada, Bull. Chem. Soc. Jpn. 47 (1974) 3006.
[28] J.W. Verhoeven, T. Scherer, B. Wegwijs, R.M. Hermant, J. Jortner, M. Bixon, S. Depaemelaere and F.C. De Schryver, Recl. Trav. Chim. Pays-Bas 114 (1995) 443.
[29] R.S. Mulliken, J. Am. Chem. Soc. 74 (1952) 811.
[30] S.J. Strickler and R.A. Berg, J. Chem. Phys. 37 (1962) 814.
[31] M. Maroncelli, R.S. Fee, C.F. Chapman and G.R. Fleming, J. Phys. Chem. 95 (1991) 1012.
[32] R.S. Fee, J.A. Milsom and M. Maroncelli, J. Phys. Chem. 95 (1991) 5170.